The utility of glass fiber-reinforced plastic orthodontic wires for clinical application

（グラスファイバー強化プラスチック製歯科矯正ワイヤーの臨床応用への有用性）

Naomi Minami

Department of Orthodontics,

Nihon University Graduate School of Dentistry at Matsudo

(Director: Prof. Kazutaka Kasai)

1. Abstract

2. Introduction

3. Materials and methods

3-1. Materials preparation

3-2. Typodonts experiment

1) Testing typodonts model preparation

2) Measurements of tooth movement in typodonts experiment

3) Strain test

3-3. Animal experiments

1) Animals

2) Application of orthodontic devices

3) Measurements of forces and change of arch width

4) Tissue preparation

5) Histomorphometrical image data processing and analysis

3-4. Statistical analysis

4. Results

4-1. Typodonts experiment

1) Change of dental arches

2) Strain test

4-2. Animal experiments

1) Measurements of force

2) Body weight during the experimental period

3) Change of arch width

4) Histological changes in periodontal tissues during tooth movement (HE staining)

5) TRAP histochemical findings

5. Discussion

6. Conclusion

7. Acknowledgments

8. References

9. Figure legends

Abstract

We have developed glass fiber-reinforced plastic (GFRP) orthodontic wire made from polycarbonate and glass fiber. The GFRP wire showed bending behavior that is similar to Ni-Ti wires and a high springback and low flexural modulus as described previously studies. The purpose of this study was to investigate the utility of the GFRP wire for clinical application using typodonts and animal experiment.

GFRP round wire with a diameter of 0.45 mm (0.018 inch.) was prepared using a diameter of 7μm glass fibers. As a control, nickel-titanium (Ni-Ti 0.018 inch) archwire were also evaluated. The typodonts model was simulated with a Class I malocclusion and mild crowding. The change in the inclination of the anterior teeth were examined by using superimposition of 3D virtual models before and after immersion. The influence of the force magnitude delivered by both wires was also investigated using a strain gauge in a maxillary anterior lateral incisor by 2.0 mm lingueoversion. The strain developed at the maxillary lateral incisors was measured immediately afterwards and 4 weeks later after ligating the wire to the brackets. In animal experiments, the maxillary second and third premolars were moved buccally for 5 weeks using 5 beagles. The change of the second and third premolar widths (P2W and P3W) in Ni-Ti and GFRP wire were investigated. Furthermore, the histological findings in periodontal ligament

(PDL) and the expression levels of the tartrate-resistant acid phosphatase (TRAP) in the alveolar bone (AB) surface were measured.

In the result of typodonts simulation, maxillary and mandibular incisors inclined labially and the arch length of the maxillary and mandibular arches incisors increased respectively after the immersion. There was no significant difference before and after simulation between the archwires ($p>0.05$). In the strain test, after ligating the wire to the brackets (from 0 week to 4 weeks), the orthodontic force of the Ni-Ti archwire decreased from 3.82 N to 3.73 N and that of the GFRP archwire decreased from 3.84 N to 3.47 N. The force of the GFRP archwires was slightly lower than that of the Ni-Ti wires. In animal experiments, the change of P2W and P3W were showed range 0.6-0.7 mm in Ni-Ti and GFRP wires. GFRP wires showed equivalent efficiency to the Ni-Ti wires in histological findings. The expression of TRAP on the compression side in the AB was increased in either group.

In conclusion, it is expected that the metal-free GFRP wire composed of polycarbonate and glass fiber is useful as an esthetically pleasing alternative to current metallic orthodontic wires.

KEY WORDS: Orthodontic wire, Fiber-reinforced composited, Typodont, strain, *In vivo* properties

Introduction

Generally, orthodontic treatment uses metallic wires made from stainless steel (SS), cobalt-chromium-nickel (Co-Cr), β-titanium (β-Ti) and nickel-titanium (Ni-Ti) alloys. [1,2]. Among these metal wires, the Ni-Ti wire is characterized as a super-elastic force, and is used for initial treatment. However, this wire is not aesthetically pleasing and may induce allergic or toxic reactions [3]. Recently, researchers have developed aesthetic orthodontic wire made from polymer-coated materials such as epoxy resin and polyethylene. However, there is potential for exfoliation of the coated layer when using these materials [4,5], and these wires may also induce metal allergy.

To resolve these issues, we developed glass fiber-reinforced plastic (GFRP) orthodontic wire made from polycarbonate and glass fiber [6,7,8]. The GFRP wire showed a bending behavior similar to Ni-Ti wire and it became clear that it has optimal and continuous force due to its high springback and low flexural modulus.

Recently, 3D virtual model analysis has been applied to measure tooth size, and width and the dental arch length, and to analyze tooth movement by mathematical superimposition of pretreatment and posttreatment models [9]. To analyze pattern of individual tooth movement and changes of arch dimension in the three-dimension (3D) spaces is a prerequisite to making a practical treatment plan. The purpose of this study

was to analyze change of the inclination of the anterior teeth and the arch dimensions in typodonts model of the Ni-Ti and GFRP archwires by using superimposition of 3D virtual models obtained before immersion (T0) and after immersion (T1). And, the force magnitude delivered by both archwires was also investigated using a strain gauge in a model simulating maxillary lateral incisor by 2.0mm lingueoversion. Furthermore, in animal experiment, the maxillary second and third premolars were moved buccally using Ni-Ti and GFRP wires for 5 weeks. The changes arch width, the histological findings in periodontal ligament (PDL) and the expression levels of the tartrate-resistant acid phosphatase (TRAP) in the alveolar bone (AB) surface were measured.

Materials and methods

Materials preparation

GFRP straight wires were fabricated using a pultrusion technique described in a previous study [6,7]. A polycarbonate (H4000; Mitsubishi Engineering-Plastics Corp., Tokyo, Japan) was used as the thermoplastic matrix because of its low melt viscosity. A glass fiber filament (Nittobo Co., Fukushima, Japan) was used as a unidirectional reinforcement for the polycarbonate matrix. GFRP round wire with a diameter of 0.45 mm (0.018 inch.) was prepared using a diameter of 7μm glass fibers. GFRP straight

wire was placed into a curved aluminium mold and then was heated at 155℃, near the glass transition point of polycarbonate, for 120 minutes to form an arch shape [6], as shown in Figure 1.

Typodonts experiment

Testing typodonts model preparation

The efficiency of tooth movement with the GFRP archwire were tested and compared with the Ni-Ti archwire. The typodonts experiment were simulated Class I malocclusion with anterior teeth crowding (DN3-RM20, Nissin, Tokyo, Japan). The brackets (slot size: 0.022) were bonded in the clinically appropriate position, which was determined according to the facial axis point using a cyanoacrylate adhesive (CC-33A; Kyowa Measuring Instruments, Inc., Tokyo, Japan) to the resin teeth on the typodonts. The size of the Ni-Ti and GFRP archwires with a diameter of 0.018 inches (Yellow Sentalloy, Tomy/GAC International, Tokyo) were inserted into the brackets, and were ligated by the elastic modules. The typodonts were submerged 30 minutes in a hot-water bath kept at about 50°C until they were completely aligned and leveled. [10].

The typodont results were obtained as the average values of 5 specimens each (n=5) [11].

Measurements of tooth movement in typodonts experiment

For the tooth movement analysis in typodonts, impressions for the maxillary and mandibular T0 and T1 of typodonts were taken using silicone impression material (DUPLICONE; Shofu Tokyo, Japan), and then dental casts were made with extra-hard plaster (New Fujirock; GC Corp, Tokyo, Japan). The dental casts were scanned by a contact-type 3D scanner, MAESTRO (MDS400; Medic Engineering Corporation, Kyoto, Japan) and interfaced to a personal computer. The inclination of the anterior teeth, arch length, arch width in both groups were measured using a three-dimensional form analysis software program (Body-Rugle; Medic Engineering Corporation, Kyoto, Japan). The reference plane in the inclination measurement of the anterior teeth is shown in Figure 2a. The inclination of the anterior teeth has been defined as the labiolingual slope of the clinical crown to the occlusal plane [12], as shown in Figure 2b. The definitions of arch length and arch width are described in Figures 2c and d. The measurements were performed by one examiner and repeated three times. The superimposition of the typodonts T0 and T1 of dental cast images were performed based on the least squares method with the metal frame of the typodonts as the immutable point [13].

Strain test

First, the strain test model used the Angle I class malocclusion model (P12-O1C; Nissin, Tokyo, Japan). The brackets type, and wire size were the same as those used in the typodonts test. The strain gauge (KFG-1-120-D16-11; Kyowa Measuring Instruments, Inc., Tokyo, Japan) was attached to the palatal surface of the maxillary left lateral incisor by the 2.0mm linguoversion using a cyanoacrylate adhesive (CC-33A, Kyowa Measuring Instruments, Inc.) (Figure 3a). The strain value induced by the Ni-Ti and GFRP arch wires were measured using a strain gauge, and a strain measuring device (DATA PLATFORM GL7000; GRAFHTEC, Tokyo, Japan) (Figure 3b). After ligating the wire to the brackets, the strain developed at the maxillary lateral incisors was measured immediately (0 weeks), and also measured after 4 weeks (4 weeks). The resulting strain values were then converted to orthodontic force. The system was maintained at a constant temperature of 37 °C in a chamber. The amount of displacement of 2 mm was expected to be the most adequate clinical setting for measuring the orthodontic force of the Ni-Ti archwire, and this setting has been the most commonly used setting in previous studies [14]. Therefore, in this experiment,

simulation was performed by setting maxillary incisor teeth displaced by the 2.0 mm lingueoversion on the model. The measurement values were obtained as the average of 10 samples (n=10).

Animals

Five beagles, periodontally healthy, each weighing 14 to 16 kg and between 13 to 16 months old (Sankyo Labo Service Co., Tokyo, Japan), were used for the experiment. The animals were caged individually with regulated light and temperature. They were fed a normal soft dog chow and had access to water ad libitum. The animal experimental protocol in this study were approved by the Ethics Committee for Animal Experiments at Nihon University School of Dentistry at Matsudo (approval no. AP15MD016). All of the dogs were performed intravenously injection with sodium propofol (Maruisi Seiyaku, Tokyo, Japan) at a dose of 25 mg/kg.

Application of orthodontic devices

The Ni-Ti sectional wires (0.018 inch) were placed on the right side (Figure 4a) and the GFRP sectional wires were placed on the left side (Figure 4b), with comparisons made to assess individual differences. The maxillary canines and fourth premolars were used as anchors, and the second and third premolars were used as the experiment teethes.

The mandibular second premolars were assigned to the as a control groups. The single brackets (slot size: 0.022) (Tomy International, Inc.) were welded to the canine bands. The second, third, and fourth premolars (micromini tube bondable, TOMY, Tokyo, Japan) were bonded with 0° offset and 0° torque. Retentive grooves were placed in the maxillary canines and second, third, and fourth premolars cusp with a high-speed handpiece and a 330-carbide bur. The teeth were then etched with 37% phosphoric acid gel for 30 seconds, and a primer was applied to each tooth. The brackets were then light-cured with transbond resin (3M Unitek, Tokyo, Japan), and the canine bands were seated with 3M Transbond XT (3M Unitek), and the resin was light-cured. Both sectional wires 0.018 inches (0.045 mm) were placed (Figures 4c and d). The maxillary second and third premolars were moved with labial tipping with both the GFRP and Ni-Ti wires for 5 weeks.

Measurements of forces and amount of tooth movement

The orthodontic force developed by the application of the Ni-Ti and GFRP wires on the second and third premolars were measured twice using a tension gauge (OHBA SIKI, Tokyo, Japan). The condition of the appliance, gingiva, and body weight change, was checked. The impression maxillary arches were taken by the silicone impression

material (Genie; Sultan, Tokyo, Japan) every week for 5 weeks, and then dental casts were made with extra-hard plaster (New Fujirock; GC Corp, Tokyo, Japan). P2W, (distance from the median palatine suture line to the cusp of the second premolars), P3W (distance from the midsagittal reference line to the cusp of the third premolars) in each Ni-Ti and GFRP wires were measured with digital calipers (Mitsutoyo, Tokyo. Japan). The measurements were performed by one examiner and repeated three times.

Tissue preparation

All 5 beagles were humanely killed after tooth movement for 5 weeks with an intravenous injection of pentobarbital (50 mg/kg). The maxillary and mandibular segments, including the canine to the fourth premolar teethes, were dissected and fixed in G-Fix (STF-01, Geno Staff, Tokyo, Japan) for 1 week. The tissue blocks (including teeth, bone and soft tissue) were then decalcified in 18% EDTA at PH 7.2 (GCM-1, Geno Staff, Tokyo, Japan) for 21 weeks at 4℃, the decalcified specimens were subsequently dehydrated using a graded ethanol series and embedded in paraffin [15]. Each sample was continuously sliced into 6-μm sections in the buccolingual direction [16]. The sections were stained with hematoxylin and eosin (HE). The sections were selected from the PDL side of one third of the apex root on the pressure side and one

third of the cervical part on the tension side of the mesial root second and third premolars [17]. Selected sections were stained with TRAP, the number of TRAP-positive (TRAP+) cells was counted on the palatal side in the bone marrow cavities immediately adjacent to the alveolar bone surface, accordance with the method of Noxon et al [18]. For TRAP positive cell, the ratio of the number of cells in each region (width: 872 μm ×height : 656 μm) was measured.

Histomorphometrical image data processing and analysis

The area 872×656 μm^2 including the maximum tension and compressed region of the mesial root in the PDL side were selected for measurement. The sections were selected from the one third of the apex root on the pressure side and one third of the cervical part on the tension side of the mesial root; one sections in each side, giving 5 measurements in total. The arbitrary hot spot was observed for each area at 200 times magnification under light microscopy. These selected image was manually traced for the Region of interest (ROI) and produced a binarized image by using Photoshop elements 11.0 (Adobe Inc. San Jose, CA). The data were cropped and were transferred to ImageJ version 1.48s. All areas of the PDL and blood vessels were measured and the blood vessel/PDL areas were calculated (Figure 5).

Statistical analyses

The experimental results was examined using a Mann Whitney test with $p < 0.05$ considered statistically significant. The error bars in the graph shows the 95% confidence interval (CI).

Result

Typodonts experiment

Amount of tooth movement

Figure 6 shows the color mapping for the superimpositions before (white) and after (green) immersion in the typodonts experiment. The crowding in the anterior region was aligned with the labial tipping in the maxillary and mandibular arch with both the Ni-Ti and GFRP archwires. These results are summarized in Tables 1. The inclination of the maxillary central incisors (U1), lateral incisors (U2) in both wires increased respectively about 7° and 11° compared with original position. Furthermore, the arch length of the maxillary and mandibular arches increased respectively about 3.1 and 3.6 mm. There was no significant difference between the Ni-Ti and GFRP archwires ($p>0.05$) (Table 2). Meanwhile, the maxillary and mandibular intercanine width (UICW, LICW), the maxillary and mandibular interfirst-molar width (UIM1W and LIM1W) were not

markedly changed (Table 2). In the arch length and arch width, there was no significant difference between the Ni-Ti and GFRP archwires.

Strain test

Figure 7a shows the orthodontic force-strain curve. After ligating the wire to the brackets (0 weeks to 4 weeks), the orthodontic force of the Ni-Ti archwire decreased from 3.82 to 3.73 N, whereas that of the GFRP archwire decreased from 3.84 to 3.47 N after the experiment. This finding shows that the strain of the GFRP wire slightly decreased compared with that of the Ni-Ti archwires after ligation (4 weeks) (p<0.05) (Figure. 7b).

Animal experiments

Measurements of force

The orthodontic force developed application of the Ni-Ti and GFRP wires to the maxillary second premolar was about 50 g, and the third premolar was about 75 g at initial force. There was no significant difference in orthodontic force in both wire (data not shown).

Body weight during the experimental period

No significant differences were observed in the body weight of the dogs between the two groups (data not shown).

Amount of the tooth movement

The increase in width of P2W and P3W in both Ni-Ti and GFRP wires showed range 0.6-0.7 mm with labial tipping. The P2W and P3W increased over five weeks in a time-dependent manner. There was no significant difference in P2W and P3W and also between Ni-Ti and GFRP wires (p>0.05) (Figures 8a and b).

Histological findings in periodontal tissues during tooth movement (HE staining)

With regard to the "tension" and "compression" areas in the second and third premolars at 5 weeks in the control group (0 g), the PDL specimens were composed of relatively dense connective tissue fibers and fibroblasts that regularly ran in a horizontal direction from the root cementum towards the AB (Figures 9a and c).

With regard to the "tension" area in the second and third premolars of the Ni-Ti and GFRP groups, the Sharpey's fibers were extended, Osteoblasts regularly arranged, and showed extensive bone remodeling at 5 weeks (Figures 9e, i, m and q). The PDL

areas in both the Ni-Ti and GFRP groups were increased compared with the control group (p<0.05) (Figure 10a). In addition, no significant difference in the area of the blood vessels was noted control and the wire groups (Figure 10b). The blood vessel/PDL areas in the wire groups were decreased compared with the control group (p<0.05) (Figure 10c). There was no significant difference in the PDL and blood vessels areas and the blood vessel/PDL areas between the wire groups.

With regard to the "compression" area in the second and third premolars in the Ni-Ti and GFRP groups, the arrangement of the Sharpey's fibers and fibroblasts became coarse and irregular, however did not show hyalinization and necrosis at 5 weeks (Figures 9g, k, o and s). The PDL areas in the Ni-Ti and GFRP groups were decreased compared with the control group (p<0.05) (Figure 11a). In addition, no significant differences in the area of the blood vessels were noted control and the wire groups (Figure 11b). The blood vessel/PDL areas in the Ni-Ti and GFRP groups were increased compared with the control group (p<0.05) (Figure 11c). No significant differences in the PDL and blood vessels areas and the blood vessels/PDL areas were noted between the wire groups.

In both the tension and compression areas, the GFRP wire showed equivalent efficiency to the Ni-Ti wire in histological changes, including the areas of the PDL,

blood vessels, and blood vessels/PDL in periodontal tissues during experimental tooth movement.

TRAP histochemical findings

In the "tension" and "compression" areas in the second and third premolars at 5 weeks in the control group (0 g), no resorption lacunae with TRAP-positive multinucleated osteoclasts were observed on the surfaces of the AB (Figures 9b and d).

In the "tension" area in the second and third premolars of the Ni-Ti and GFRP groups, on the surface of the AB, no resorption lacunae with TRAP-positive multinucleate osteoclasts were observed at 5 weeks (Figures 9f, j, n and r).

With regard to the "compression" area in the second and third premolars of the Ni-Ti and GFRP groups, on the surface of the AB, resorption lacunae with multinucleate TRAP-positive osteoclasts were observed at 5 weeks (Figures 9h, l, p and t). The expression of TRAP in the compression side on the surface of the AB was significantly increased at 5 weeks (Figure 11d). A quantitative evaluation showed that the number of TRAP-positive osteoclasts was roughly equal for both wire groups (Figures 10d and 11d).

Discussion

In our previous studies, aesthetic orthodontic wire made from GFRP composed of glass fiber and polycarbonate was developed using pultrusion. As the next step in preparing to use this wire in clinical orthodontic treatment, we investigated that the effect of GFRP wire on the alignment in the typodont model simulating. There was no significant difference after immersion in the maxillary and mandibular between the Ni-Ti and GFRP archwires (Figure 6). Therefore, the GFRP archwires were found to exhibit similar behavior as Ni-Ti archwires during the initial leveling stage. The force magnitudes regarding the strain of the Ni-Ti and GFRP archwires were examined using a strain gauge. Tochigi et al. [14] investigated the orthodontic force magnitude delivered by Ni-Ti archwires in a simulation of mandibular lateral incisor lingual version. The strain force magnitude was 2.44 N in 0.014-inch and 3.61 in 0.016-inch Ni-Ti archwires. In addition, Miura et al. [19] reported that the orthodontic force of 0.018-inch Ni-Ti wire ranged from 2.0 to 4.4 N. These reports show that the strain forces of Ni-Ti and GFRP wires in this study were not excessive strain forces, but were optimal orthodontic forces. After ligating the wire to the brackets (4 weeks), the orthodontic force developed by application of the GFRP archwire slightly decreased, compared with that of the Ni-Ti archwires. Reduction in orthodontic force in GFRP archwire shows slight deformation,

the glass fiber crack and polycarbonate deformation occurred.

Parvizi and Rock [20] asserted that full recovery on unloading might not always be obtained and had been shown to lie in the range 89-94 per cent with Ni-Ti wire. While the GFRP wire may not have had sufficient recovery of the initial configuration, an orthodontist typically changes the Ni-Ti wire every one to two months in the initial leveling stage [19]. Therefore, the deformation of GFRP archwire over 4 weeks will not markedly influence the apparatus, and the wire will still be effective in relieving crowding.

We investigated the GFRP wire measurement of the orthodontic force and the changes of P2W and P3W compared with the Ni-Ti wire *in vivo*. Owens et al [21]. suggested that the differences in the size and anatomy of the PDL and the AB between dogs and humans are rather small, we performed this experiments in dogs. There was no significant difference in orthodontic force P2W and 3PW in both wire. Furthermore, the changes of P2W and 3PW were similar between the two wires (Figure 8).

Pilon et al. [22]. showed that 50 g of optimal force application produced significantly greater tooth movement with significantly less root resorption over a period of 120 days in relation to a heavier force application in dogs. In other words, this model supports it as showing efficient teeth movement. Iino et al. [23] shows that the

amount of tooth movement by an orthodontic force of 50 g was 1.0 mm in 4 weeks. These previous studies support the results in the present study. Furthermore, we examined the histological findings of periodontal tissue during tooth movement. Our histological findings were similar to those of previous studies. In the “tension” side, Tsuge et al. [24] demonstrated that the total cross-sectional area of the PDL at 7 days was significant larger in their experimental group than in control groups in a rat model of tooth movement. In addition, the total cross-sectional areas of the blood vessels were not decreased, while the ratio of blood vessels to PDL was significantly decreased after orthodontic force loading. In contrast, with regard to the “compression” side, Noda et al. [25] demonstrated that light force maintained the vascular structure in a rat model of tooth movement, and concluded that a heavier force, partial or total occlusion of vessels, resulting in degeneration or necrosis of the PDL. Krishnan et al. [26] suggested that depending on the magnitude of applied force, the reaction at this site differs; light pressure produced direct bone resorption and heavy forces produce hyalinization. In the results of this study, there was no significant difference in histological findings between the two wire types. To maintain the biological activity of compressed PDL, a compressed condition without obstructing blood circulation was maintained during efficient tooth movement. Therefore, GFRP wire showed equivalent efficiency to Ni-Ti

wire with regard to histological changes during tooth movement.

In this study, we examined approximately 0.018-inch diameter GFRP wire. Generally, a narrower-diameter rod, such as 0.014- or 0.016-inch diameter, is used at the beginning of clinical orthodontic treatment. Future studies should investigate the effects of these narrow diameters of GFRP wire for further clinical application.

In conclusion, it is expected that this metal-free GFRP wire composed of polycarbonate and glass fiber to be useful as an esthetically pleasing alternative to current metallic orthodontic wires.

Acknowledgments

This article is based on a main reference paper titled, “The effects of glass fiber-reinforced plastic for orthodontic wire on bone remodeling during experimental tooth movement: histological study in dogs.” in press at the *International Journal of Oral-Medical Sciences*, and reference paper titled, “The effects of glass fiber-reinforced plastic for orthodontic wire on the malocclusion of mild anterior crowding during the initial leveling stage: A typodont experimental study” in press at the *Orthodontic waves.*

References

【1】 Eliades T. Dental materials in orthodontics. In: Graber LW, Vanarsdall Jr. RL, Vig KWL, editors. Orthodontics: current principles and techniques, 5th ed. Philadelphia, PA: Elsevier/Mosby; 2012. 1023-1037.

【2】 O'Brien WJ. Orthodontic wire. In: O'Brien WJ editor. Dental materials and their selection, 4th ed. Chicago: Quintessence Pubrishing, 2008. p. 276-292.

【3】 Eliades T, Athanasiou AE. In vivo aging orthodontic alloys: implication for corrosion potential, nickel release, and biocompatibility. Angle Orthod 2002;72:222-237.

【4】 Elayyan F, Silikas N, Bearn D. Ex vivo surface and mechanical properties of coated orthodontic archwires. Eur J Orthod. 2008;30:661-667.

【5】 Da Silva DL, Mattos CT, Simão RA, de Oliveria Ruellas AC. Coating stability and surface characteristics of esthetic orthodontic coated archwire. Angle Orthod 2013;89:994-1001.

【6】 Tanimoto Y, Inami T, Yamaguchi M, Nishiyama N, Kasai K. Preparation, mechanical, and in vitro properties of glass fiber-reinforced polycarbonate composites for orthodontic application. J Biomed Mater Res B Appl Biomater 2015;103:743-750.

【7】 Inami T, Tanimoto Y, Yamaguchi M, Shibata Y, Nishiyama N, Kasai K. Surface topography, hardness, and frictional properties of GFRP for esthetic orthodontic wires. J Biomed Mater Res B Appl Biomater 2016;104:88-95.

【8】 Inami T, Tanimoto Y, Minami N, Yamaguchi M, Kasai K. Color stability of laboratory glass –fiber-reinforced plastics for esthetic orthodontics wires. Korean J Orthod 2015;45:130-135.

【9】 Cha BK, Lee JY, Jost-Brinkmann PG, Yoshida N. Analysis of tooth movement in extraction cases using three-dimensional reverse engineering technology. Eur J Orthod 2007;29:325-331.

【10】 Lee RJ, Pham J, Choy M, Weissheimer A, Dougherty HL Jr, Sameshima GT, et al. Monitoring of typodont root movement via crown superimposition of single cone-beam computed tomography and consecutive intraoral scans. Am J Orthod Dentofacial Orthop 2014;145:399-409.

【11】 Shen G, Chen RJ, Hu Z, Qian YF. The effects of a newly designed twin-slot bracket on severely malpositioned teeth-a typodont experimental study. Eur J Orthod 2008;30:401-406.

【12】 Cho MY, Choi JH, Lee SP, Baek SH. Three-dimensional analysis of the tooth movement and arch dimension changes in Class I malocclusions treated with first premolar extractions: A guideline for virtual treatment planning. Am J Orthod Dentofacial Orthop 2010;138:747-757.

【13】 Yanagida H, Koga Y, Rokutanda H, Tominaga J Yoshida N. Qualitative and quantitative evaluation of central incisor movement by integration of three-dimensional images of dental cast and cephalogram. Orthodontic waves, 2015;74:62-68.

【14】 Tochigi K, ODA S, Arai K. Influences of archwire size and ligation method on the force magnitude delivered by nickel-titanium alloy archwires in a simulation of mandibular right lateral incisor linguoversion. Dent Mater J 2015;34:388-393.

【15】 Lv T, Kang N, Wang C, Han X, Chen Y, Bai D. Biologic response of rapid tooth movement with periodontal ligament distraction. Am J Orhtod Dentofacial Orthop 2009;136:401-411.

【16】 Ruso S, Campbell PM, Rossmann J, Opperman LA, Taylor RW, Buschang PH. Bone response to buccal tooth movements-with and without flapless alveolar decortication. Eur J Orthod 2014;36:613-623.

【17】 Kraus CD, Campbell PM, Spears R, Taylor RW, Buschang PH. Bony adaptation after expansion with light-to-moderate continuous forces. Am J Orthod Dentofacial Orthop 2014;145:655-666.

【18】 Noxon SJ, King GJ, Gu G, Huang G.Osteoclast clearance from periodontal tissues during orthodontic tooth movement. Am J Orthod Dentofacial Orthop 2001;120:466-476.

【19】 Miura F, Mogi M, Ohura Y, Hamanaka H. The superelastic property of the Japanese NiTi alloy wire for use in orthodontics. Am J Orthod Dentofacial Orthop 1986;90:1-10.

【20】 Parvizi F, Rock WP. The load/deflection characteristics of thermally activated orthodontic archwires. Eur J Orthod 2003;25:417-421.

【21】 Owens SE, Buschang PH, Cope JB, Franco PF, Rossouw PE. Experimental evaluation of tooth movement in the beagle dog with the mini-screw implant for orthodontic anchorage. Am J Orthod Dentofacial Orthop. 2007;132:639-646.

【22】 Pilon JJ, Kuijpers-Jagtman AM, Maltha JC. Magnitude of orthodontic forces and rate of bodily tooth movement. An experimental study. Am J Orthod Dentofacial Orthop 1996;110:16-23.

【23】Iino S, Sakoda S, Ito G, Nishimori T, Ikeda T, Miyawaki S. Acceleration of orthodontic tooth movement by alveolar corticotomy in the dog. Am J Orthod Dentofacial Orthop 2007;131:448.e1-8.

【24】Tsuge A, Noda K, Nakamura Y. Early tissue reaction in the tension zone of PDL during orthodontic tooth movement. Arch Oral Biol 2016;65:17-25.

【25】Noda K, Nakamura Y, Kogure K, Nomura Y. Morphological changes in the rat periodontal ligament and its vascularity after experimental tooth movement using superelastic forces. Eur J Orthod 2009;31:37-45.

【26】Krishnan V, Davidovitch Z. Cellular, molecular, and tissue-level reactions to orthodontic force. Am J Orthod Dentofacial Orthop 2006;129:469 el-32.

Figure legend

Figure 1. (a) Preparation of commercial Ni-Ti arch wires, (b) Preparation of Esthetic GFRP orthodontic arch wires.

Figure 2. The reference plane in the inclination measurement of the anterior teeth and the definitions of arch dimension. (a) The gray plane is setting of parallel to the occlusal plane. (b) The inclination of the anterior teeth has been defined as the labiolingual slope of the clinical crown to the occlusal plane. (c) Maxillary arch width (d) Mandibular arch width. ICW; intercanine width (distance between the cusp tip of the right and left canines) IM1W; interfirst molar width (distance between the mesio buccal cusp tip of right and left first molars) AL; arch length (distance between the midpoint of the incisal edges of the bilateral incisors and a line connecting the bilateral first molar buccal cusp). U1; Maxillary central incisor U2; Maxillary lateral incisor L1; Mandibular central incisor L2; Mandibular lateral incisor

Figure 3. Experimental set-up for strain test. (a) The strain gauge was attached to the palatal surface of the maxillary left lateral incisor of the 2.0mm linguoversion by using a cyanoacrylate adhesive. (b) The strain values of the NI-Ti and GFRP wires were measured by using a dynamic strain measuring instrument and software, with interfaced to a personal computer.

Figure 4. (a) A Ni-Ti wire was placed on the right side. (b) A GFRP wire was placed on the left side. (c) Occlusal views, the both wire 0.018 inches (0.45 mm) inserted into the buccal tube, from canine to fourth premolar.

(d) Illustration of the orthodontic appliance applying optimal force. The green line indicates the median palatine suture line. The blue arrow indicates the second premolar width (P2W), (distance from the median palatine suture line to the cusp of the second premolars) and the red arrow indicates the third premolar width (P3W), (distance from the median palatine suture line to the cusp of the third premolars) in each Ni-Ti and GFRP wires were measured with digital calipers (Mitsutoyo, Tokyo. Japan). The measurements were performed by one examiner and repeated three times.

Figure 5. (a) Images of measurement area with hematoxylin and eosin staining D; dentine, B; bone. (b) Extracted computer-processing image of the PDL and vascular cross-sectional areas. Black-colored area shows the PDL cross section and white circles shows the blood vessels.

Figure 6 The 3D superimposition of the typodonts before immersion (T0) and after immersion (T1) of dental cast images were performed by means of the least squares method. (a) NiTi occlusal view (b) GFRP occlusal view.

Figure 7. (a) The orthodontic force-strain curve. The result of converting by orthodontic force-strain curve expressed in both wires. (b) The orthodontic force magnitude of these wires after ligating wire for 0week and 4 weeks. The orthodontic force of the GFRP wires were slightly decreased than that of Ni-Ti wires after ligating wire (4 weeks) ($P<0.05$).

Figure 8. Buccal tooth movements of the maxillary second and third premolars on the Ni-Ti and GFRP wires measured digital caliper. The error bars in the

graph shows the 95% confidence interval (CI). (a) the second premolar, (b) the third premolar

Figure 9. Light microscopy images shows the histological findings in periodontal tissues during buccal tooth movement in the second and third premolars with Ni-Ti and GFRP wires. (Hematoxylin and eosin staining and TRAP stainings, ×200) The arrows head indicate the osteoclasts on the alveolar bone by the compression side. B; Bone, PDL; Periodontal ligament, C; cementum, D; dentin. Scale bar = 50μm. The direction of the applied force is indicated by the large arrow.

Figure 10. Histomorphometry by the tension side in the second and third premolars. (a) The area of the periodontal ligament, (b) the area of the blood vessels, (c) The blood vessel/PDL areas, (d) The amount of TRAP positive (TRAP+) cells were counted by the tension side and in the bone marrow cavities immediately adjacent to the alveolar bone surface ($p<0.05$). The error bars in the graph shows the 95% confidence interval (CI).

Figure 11. Histomorphometry by the compression side in the second and third premolars. (a) the area of the periodontal ligament, (b) the area of the blood vessels, (c) The blood vessel/PDL areas, (d) The amount of TRAP positive (TRAP+) cells were counted by the compression side and in the bone marrow cavities immediately adjacent to the alveolar bone surface ($p<0.05$). The error bars in the graph shows the 95% confidence interval (CI).

Table 1. Comparison of Inclination of the anterior teeth between T0 and T1 in typodonts.

Table 2. Comparison of Arch length and Arch width between T0 and T1 in typodonts.

(a) Ni-Ti wire

(b) GFRP wire

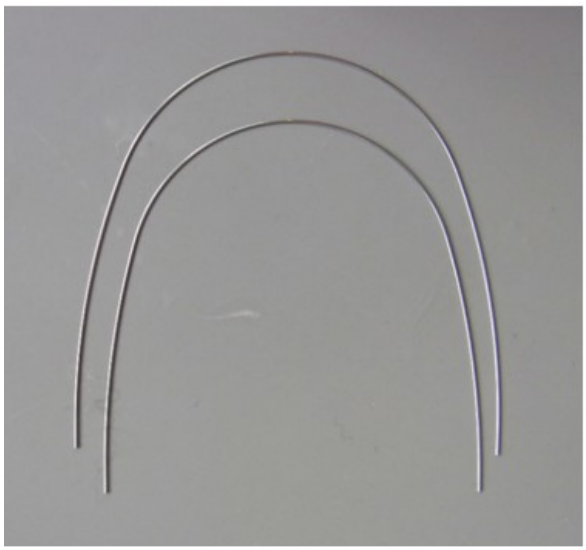

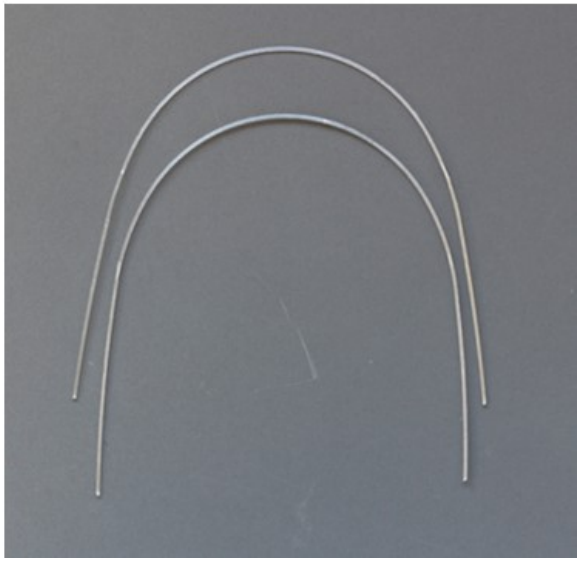

Figure 1

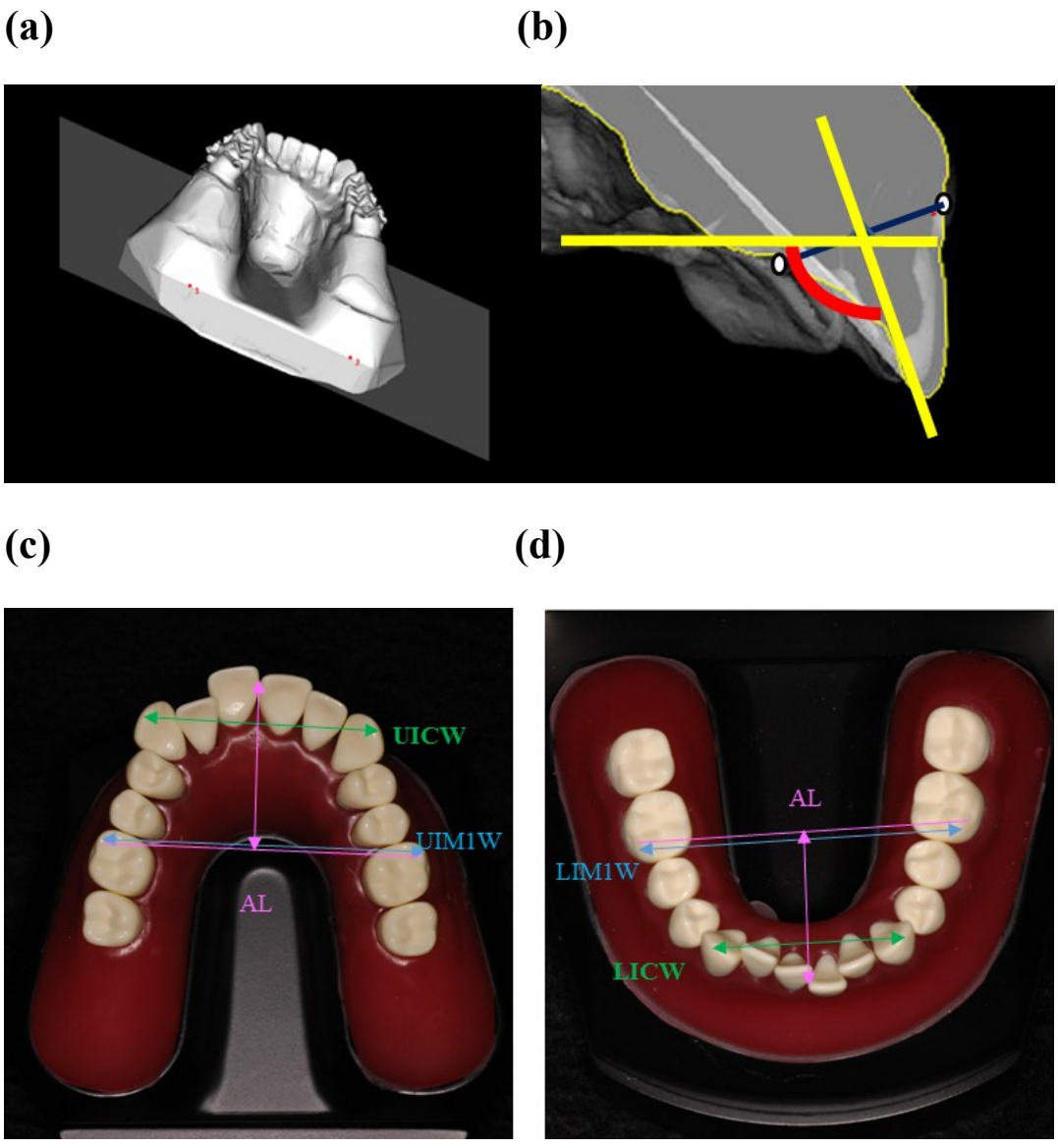

Figure 2

(a)

(b)

Figure 3

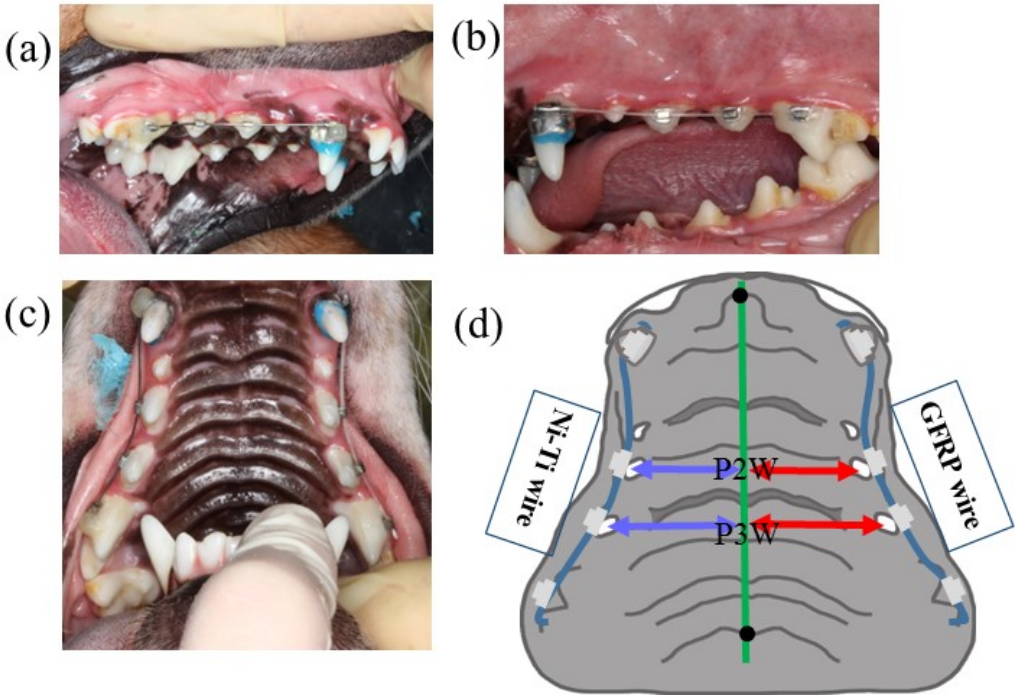

Figure 4

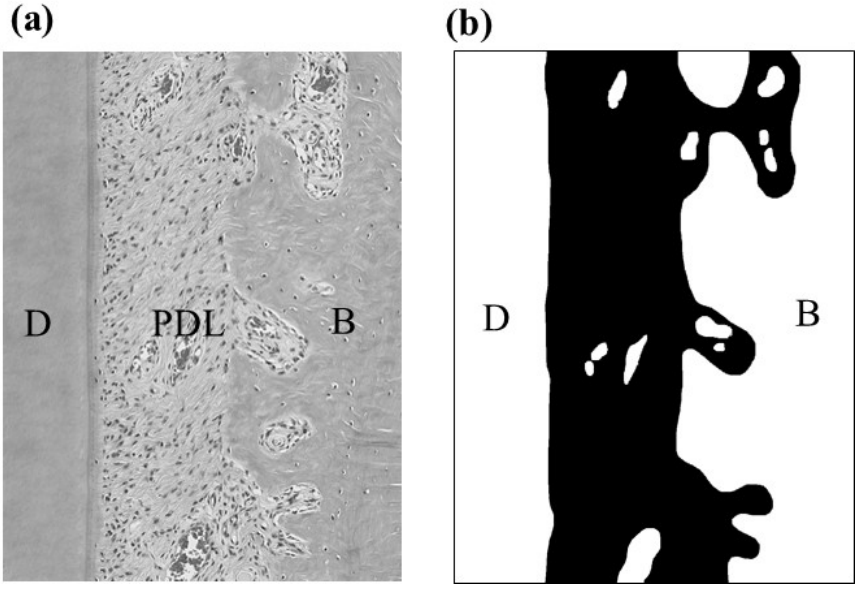

Figure 5

(a)

Ni-Ti

Maxillary

Mandibular

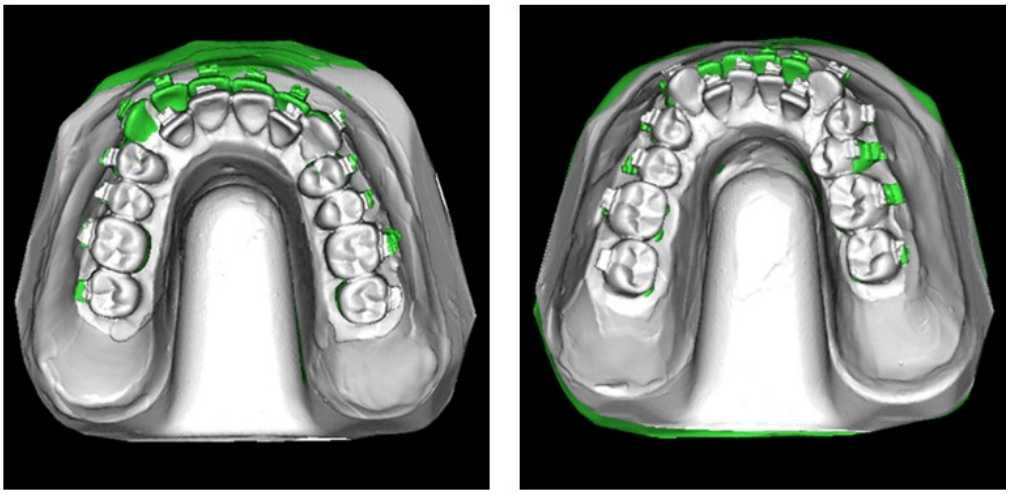

(b)

GFRP

Maxillary

Mandibular

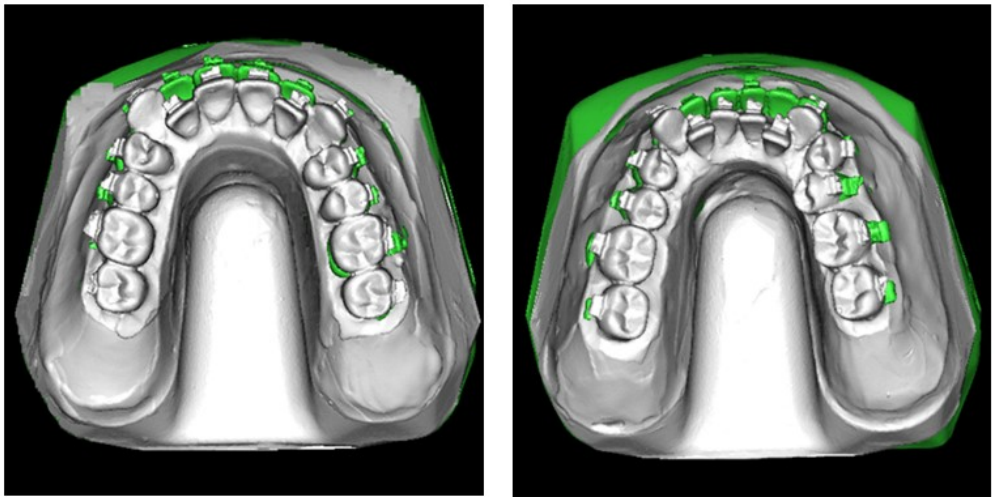

Figure 6

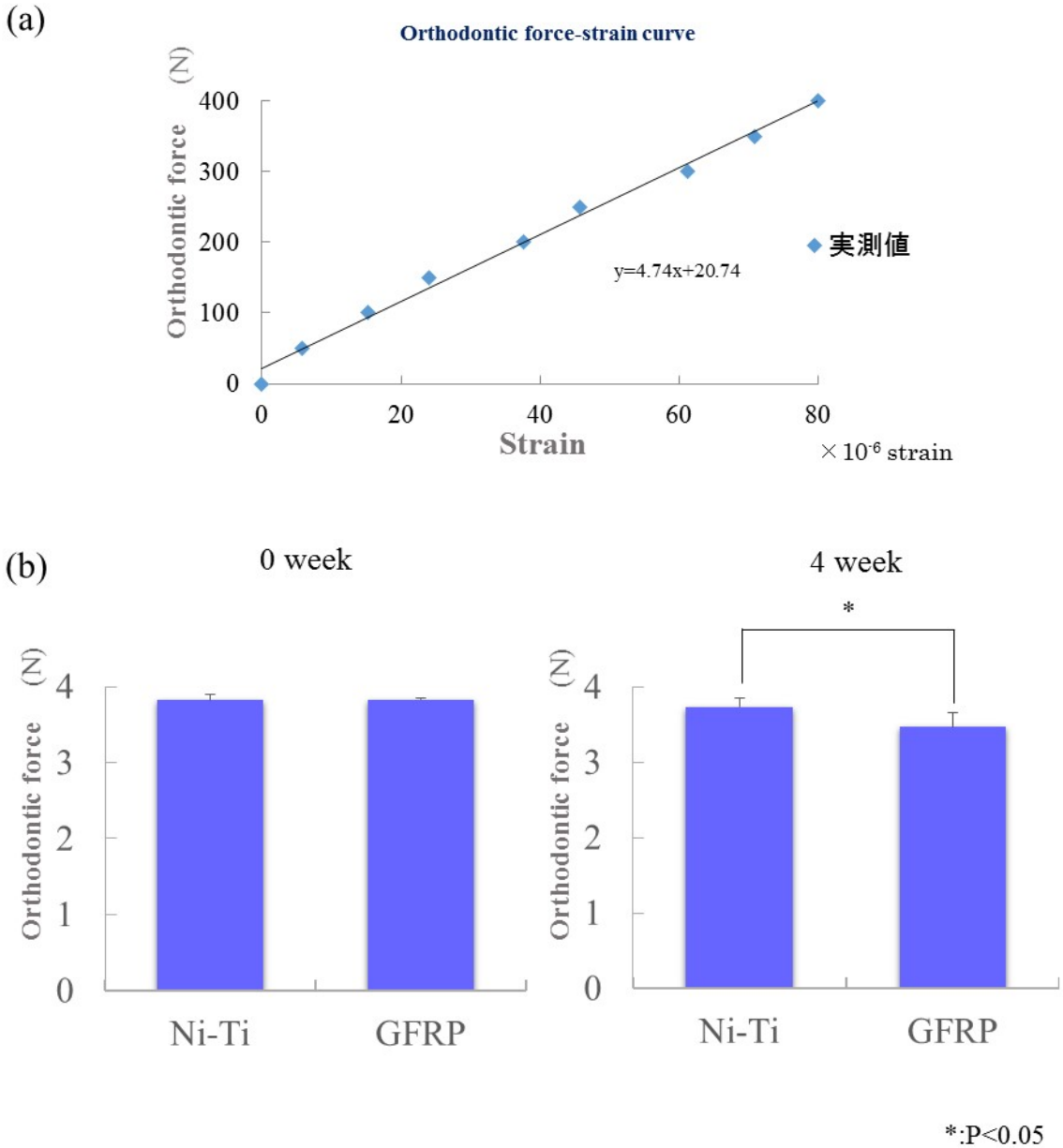
(a)
Orthodontic force-strain curve
Orthodontic force (N)
400
300
200
100
0
0
20
40
60
80
Strain
× 10-6 strain
y=4.74x+20.74
実測値
(b)
0 week
4 week
*
Orthodontic force (N)
4
3
2
1
0
Ni-Ti
GFRP
*:P<0.05

Figure 7

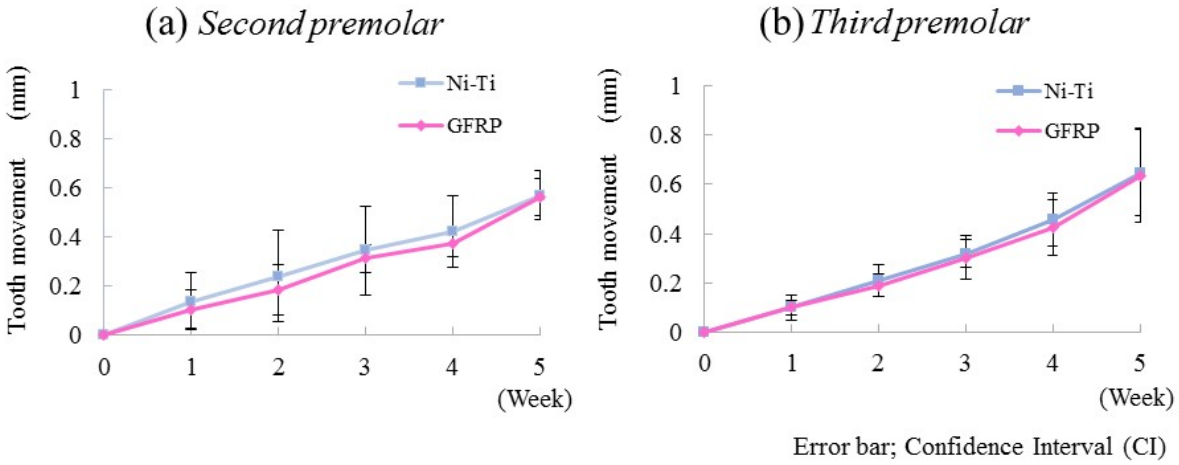
(a) Second premolar
(b) Third premolar
Tooth movement (mm)
Ni-Ti
GFRP
(Week)
Error bar; Confidence Interval (CI)

Figure 8

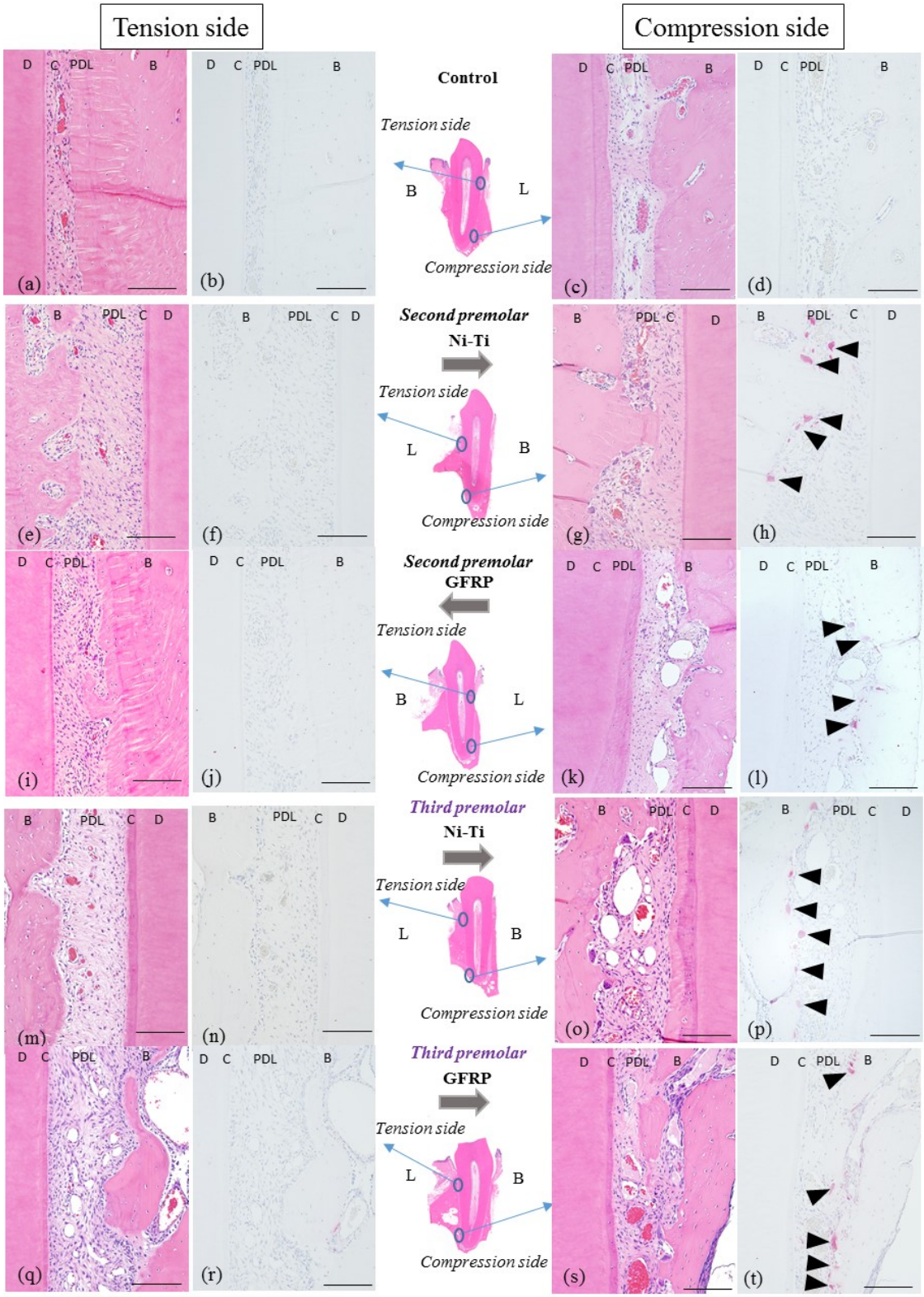
Tension side
Compression side
Control
Tension side
B
L
Compression side
Second premolar
Ni-Ti
Tension side
L
B
Compression side
Second premolar
GFRP
Tension side
B
L
Compression side
Third premolar
Ni-Ti
Tension side
L
B
Compression side
Third premolar
GFRP
Tension side
L
B
Compression side
D C PDL B
B PDL C D
(a)
(b)
(c)
(d)
(e)
(f)
(g)
(h)
(i)
(j)
(k)
(l)
(m)
(n)
(o)
(p)
(q)
(r)
(s)
(t)

Figure 9

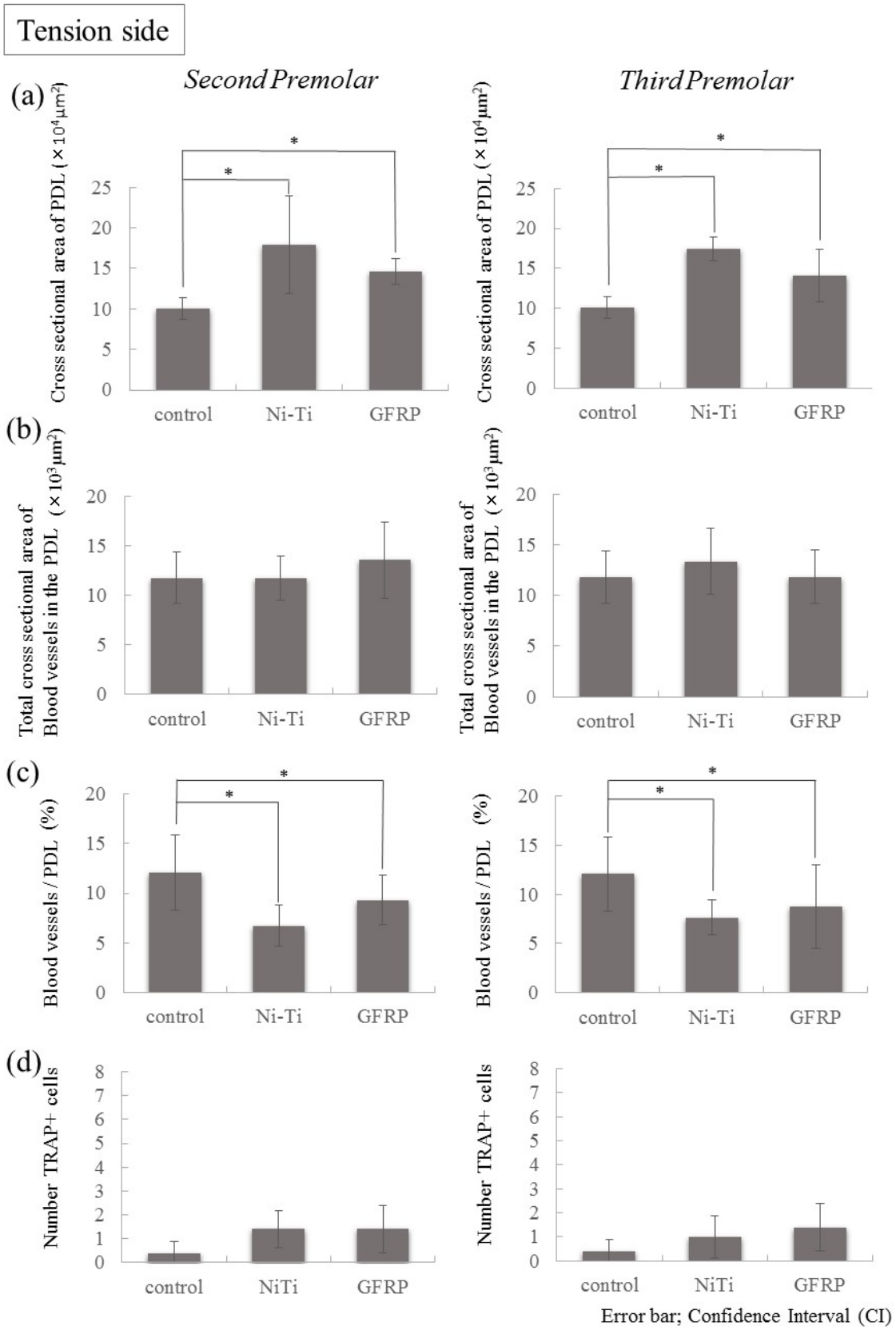
Tension side
Second Premolar
Third Premolar
(a)
Cross sectional area of PDL (×10⁴μm²)
(b)
Total cross sectional area of Blood vessels in the PDL (×10³μm²)
(c)
Blood vessels / PDL (%)
(d)
Number TRAP+ cells
control
Ni-Ti
NiTi
GFRP
*
Error bar; Confidence Interval (CI)

Figure 10

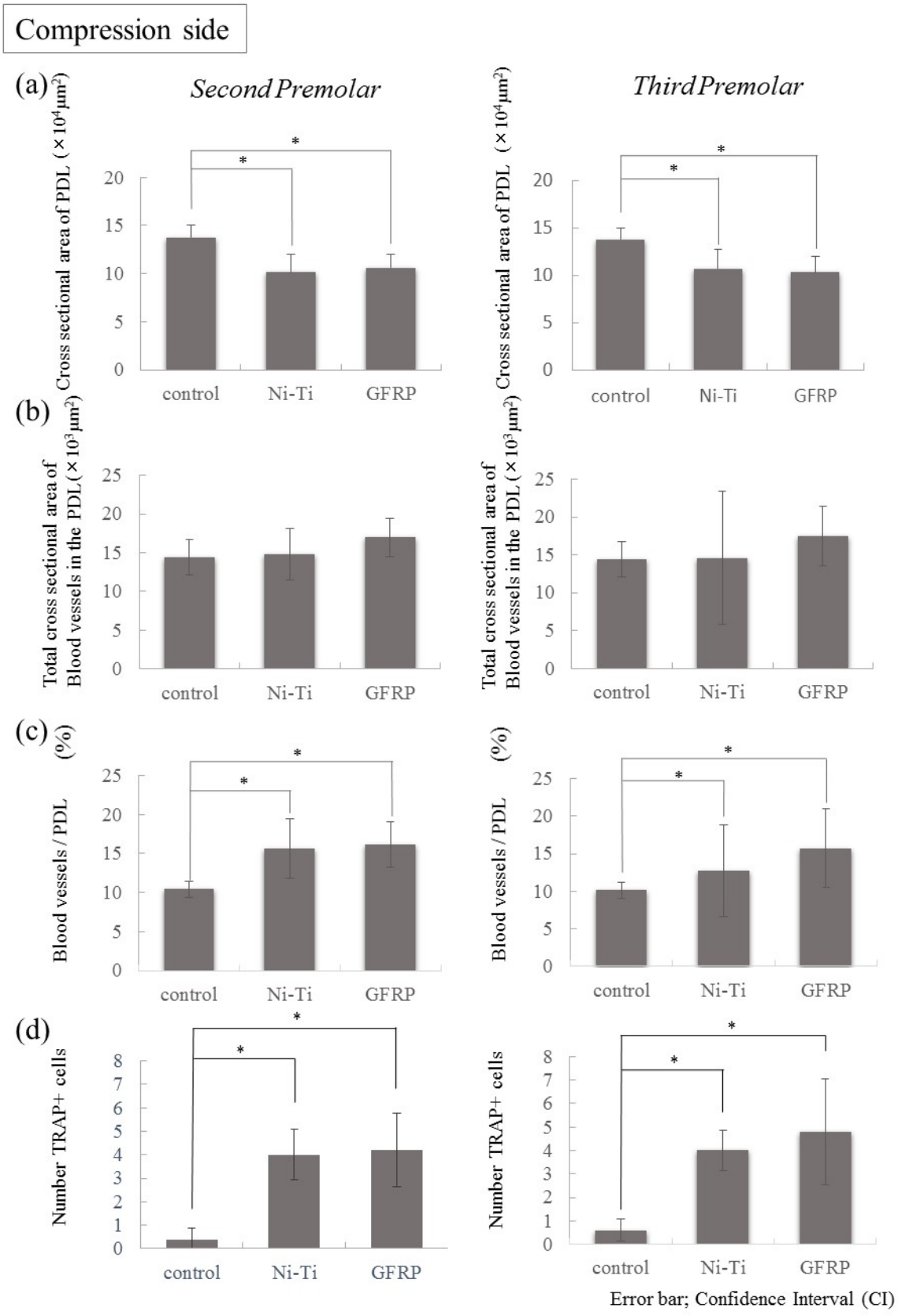
Compression side
(a)
Second Premolar
Third Premolar
Cross sectional area of PDL (×10⁴μm²)
(b)
Total cross sectional area of Blood vessels in the PDL (×10³μm²)
(c)
Blood vessels / PDL (%)
(d)
Number TRAP+ cells
control
Ni-Ti
GFRP
Error bar; Confidence Interval (CI)

Figure 11

Table.1 Comparison of inclination of the anterior teeth, between T0 and T1 in the typodonts

			Ni-Ti wire	GFRP wire	T0-T1		Ni-Ti VS
		(T0)	(T1)	(T1)	Ni-Ti	GFRP	GFRP
Inclination	U1	105.8°	113.6°	112.2°	*	*	NS
	U2	100.2°	112.9°	111°	*	*	NS
	L1	98.1°	107.1°	106.1°	*	*	NS
	L2	90.2°	104.2°	102.7°	*	*	NS

Inclination; labioversion (+) or linguoverson (-) *P＜0.05

NS: Not significant

U1: maxillary central incisor, U2: maxillary lateral incisor, L1: mandibular central incisor,

L2: mandibular lateral incisor,

Table.2 Comparison of arch length and arch width between T0 and T1 in the typodonts

			Ni-Ti wire	GFRP wire	T0-T1		Ni-Ti VS
		(T0)	(T1)	(T1)	Ni-Ti	GFRP	GFRP
Arch width	U1CW	36.9mm	36.89mm	36.96mm	NS	NS	NS
	U1MW	51.40mm	51.50mm	51.50mm	NS	NS	NS
	L1CW	28.30mm	28.70mm	28.60mm	NS	NS	NS
	L1MW	42.70mm	42.90mm	42.90mm	NS	NS	NS
Arch length	Maxillary	34.20mm	37.3mm	37.2mm	*	*	NS
	Mandibular	30.10mm	33.8mm	33.7mm	*	*	NS

*P＜0.05

Arch length; increase (+) or decrease (-) NS: Not significant

Arch width; increase (+) or decrease (-)

T0; before immersion in Typodonts

T1:after immersion in Typodonts

U1: maxillary central incisor, U2: maxillary lateral incisor, L1: mandibular central incisor,

L2: mandibular lateral incisor, UICW; maxillary intercanine width, LICW; mandibular intercanine width,

UIM2W; maxillary interfirst molar width, LIM1W, mandibular interfirst molar width